Journal of Constructional Steel Research 220 (2024) 108851

Contents lists available at ScienceDirect

Journal of Constructional Steel Research

journal homepage: www.elsevier.com/locate/jcsr

Experimental investigation of welded steel T-stub components under high loading rates

Grace Kendall, Artem Belyi, Ahmed Elkady *

Department of Civil, Maritime and Environmental Engineering, University of Southampton, Burgess Road, Boldrewood Campus, Southampton SO17 7QF, UK

ARTICLE INFO

Keywords:
Steel T-stub
Strain rate
Loading rate
Connection ductility
Bolt preload

ABSTRACT

The equivalent steel T-stub approach is widely used in practice to analyse and design bolted steel joints that are otherwise complex to study. The available analytical and empirical models for characterizing the response of T-stub components are based on numerous experimental and numerical research studies. This research is mostly concerned with the pseudo-static response of the T-stub. However, natural and man-made hazards (such as earthquakes and impacts) are dynamic. Considering the strain-rate sensitivity of steel, dynamic effects may have a notable effect on structural behaviour. A limited number of studies investigated the response of steel components/joints at high loading rates with inconclusive, and sometimes conflicting, observations. Accordingly, an experimental study is undertaken to address the data shortage. A total of 57 welded steel T-stubs were tested under monotonic tension. The main test parameters included the T-stub flange plate thickness, the loading rate, and the bolt preload condition. The test data underscored the influence of the loading rate and bolt preload. Notably, at a loading rate of 50 mm/s, an average of 35% reduction in the elastic stiffness, a 5% amplification of strength, and a 22% reduction in ductility is observed compared to the reference pseudo-static loading rate. The paper discusses the test observations in detail, evaluates the findings considering past research, and assesses potential implications on design.

1. Introduction

The current design paradigm relies on tuning the relative strength and stiffness of the different joint and connection components (column, beam, endplate, angle cleat, bolts, and welds) to achieve the target rigidity, maintain a hierarchal –ductile- progression of damage, and avoid early brittle failure modes (e.g., weld failure and bolt rupture). To study bolted steel connections and particularly semi-rigid ones, the connection is discretised into an assembly of T-stub components. This is illustrated in Fig. 1 which shows a few equivalent T-stubs extracted from common bolted steel connections. Steel T-stubs can be divided into two main categories: welded and hot-rolled. Welded T-stubs represent components such as the beam to endplate components while hot-rolled T-stubs represent components such as the column flange and angle cleats. Understanding, and consequently accurately predicting, the behaviour of steel T-stubs is fundamental in computing the stiffness, strength and ductility of steel joints, as part of analytical and mechanical methodologies [1].

Current analytical and empirical methods for characterizing the mechanical response parameters of steel T-stubs under tension are based on decades of numerous experimental research studies. These studies mostly involved pseudo-static loading conditions, where displacements/forces are applied at a very low rate (typical loading speed <1 mm/s or a strain rate $<10^{-3}$ s^{-1}). Although pseudo-static tests are convenient, they are not a true representation of real hazards (earthquakes, collisions, explosions, column loss, etc.) which are dynamic. These dynamic hazards exert inertia loads on structures, amplify the shear force demands in structural members and components and accentuate the material's strain rate ($\dot{\varepsilon}$) sensitivity. For the latter, steel is a particularly strain-rate sensitive construction material, where high strain rates can amplify the yield and ultimate stress by up to 50% and 20%, respectively [2–5]. Most critically, a reduction in fracture strain and fracture toughness (i.e., material ductility) of up to 50% is observed, particularly in high-strength steel grades, which increases the risk of bolt and weld failure [6–9].

Concerning bolted joints, dynamic loading may likely trigger connection slippage and induce larger shearing forces on bolts; thereby leading to unfavourable brittle failure modes [10,11]. This is also

* Corresponding author.
E-mail addresses: gck1g21@soton.ac.uk (G. Kendall), ab1u20@soton.ac.uk (A. Belyi), a.elkady@soton.ac.u (A. Elkady).

https://doi.org/10.1016/j.jcsr.2024.108851
Received 16 May 2024; Received in revised form 10 June 2024; Accepted 17 June 2024
Available online 21 June 2024

dependent on the amount of bolt preload, which controls the connection's ability to resist shear forces through friction and consequently the amount of slippage and the percentage of shear load transfer through the bolt shearing and plate hole bearing [2]. These phenomena can potentially lead to an unfavourable deviation from the failure mode stipulated in the design process. This threatens global structural robustness and can trigger progressive collapse. This issue becomes more critical knowing that several researchers noted that the current design codes and available predictive numerical models, can sometimes be unreliable in predicting the pseudo-static connection response parameters and deformation modes [12,13]. This may be exacerbated under realistic dynamic loading. For instance, recent tests [14] showed that the current Eurocode 3 [1] design overpredicts the connection strength by about 30% under high loading rates.

While testing full-scale bolted joints at high loading rates is costly, testing T-stub components is not and can provide equally valuable insights. Nonetheless, while hundreds of T-stubs were tested in the literature, a limited number of those were tested at high loading rates. The findings from these limited tests although useful are not conclusive and sometimes contradictory. Dinu et al. [15] tested welded T-stubs under loading rates ranging from 0.05 to 10 mm/s. They noted a small influence of the loading rate on the ultimate capacity, ductility, and failure mode. Baldassino et al. [16] tested welded and hot-rolled T-stubs, with 10 mm and 16 mm flange plates, at loading rates ranging between 0.07 mm/s and 326 mm/s. The tests also showed limited influence on load capacity and ductility but noted the importance of the weld quality to prevent brittle failures. Relevant test data on bolted lap components in tension and shear noted the increase in strength, reduction in ductility and the significant effect of loading rate on slippage in friction-type connections [2,15]. Others also reported a 2–6% increase in ultimate loads accompanied by an 8% to 9% increase in ductility [17]. Furthermore, available tests suggest that bolt preload provides significant enhancements in the initial stiffness, increasing it by up to three times compared to snug-tight T-stub connections [18–20]. Zhang et al. [18] further noted that bolt preload significantly enhanced the deformation capacity by 27%. Finally, the limited number of full-scale joints tested under high loading rates showed that under dynamic loading, some specimens experienced an increase in strength/stiffness and reduction in ductility coupled with large shear-to-flexural force ratios, while others had limited strength due to the early onset of bolt thread stripping [14,21–23]. Relevant tests on welded connections [24–27] reported a 10% to 20% strength amplification but inconclusive observations on ductility.

To complement the existing experimental data in the literature and help draw a clearer understanding, 57 welded T-stub specimens are tested as part of this study. The focus is to investigate both the loading rate and bolt preload effects on the T-stub response. The subsequent sections describe the test parameters, and the test setup, followed by a discussion of the observed deformation modes and the individual and combined effect of the test parameters on the elastic stiffness, strength, and ductility.

2. Experimental Study

2.1. Test specimens and parameters

A total of 57 welded T-stub specimens were tested. Table 1 summarizes the geometric and loading parameters of the test specimens. The specimens are labelled using the following notation: **T***x*-*y*, where *x* is the number of bolts and *y* is the flange plate thickness (t_f). Specifically, two bolt layouts are considered: T2 and T4. T2 involves a single bolt row with two bolt columns layout and T4 involves a two bolt rows by two bolt columns layout, as illustrated in Fig. 2. All T-stubs had a flange width (b_f), of 220 mm and M16 Grade 8.8 bright zinc-plated steel bolts [28]. The T2 and T4 specimens had a plate length (L_f) equal to 80 mm and 150 mm, respectively. Referring to Fig. 2, most T-stubs had a bolt gauge distance (g) of 120 mm and were tested in a T-stub-on-rigid support assembly configuration. Two specimen groups employed variations of the T2–10 specimen. Those involved one group with larger L_f = 120 mm (labelled as T2–10-120) and another with a double T-stub assembly configuration (see Fig. 2) and g = 180 mm (labelled T2–10D). The specimens' geometry differs primarily in terms of t_f which ranges from 6 mm to 20 mm, and L_f which ranges from 80 mm to 150 mm. The specimens are subjected to different monotonic tensile loading rates ranging from pseudo-static 0.05 mm/s to dynamic 100 mm/s. The selected loading rates are consistent with those used in the literature which represent those expected under gravity-driven progressive collapse scenarios [29]. Finally, two bolt-preload conditions are considered: snug-tight (ST) and full-preloaded (FT).

All plates are fabricated from grade S275 steel. The material properties are described in the next section. Fillet welding is used to join the web and flange plates. The weld size (s) is summarized in Table 1.

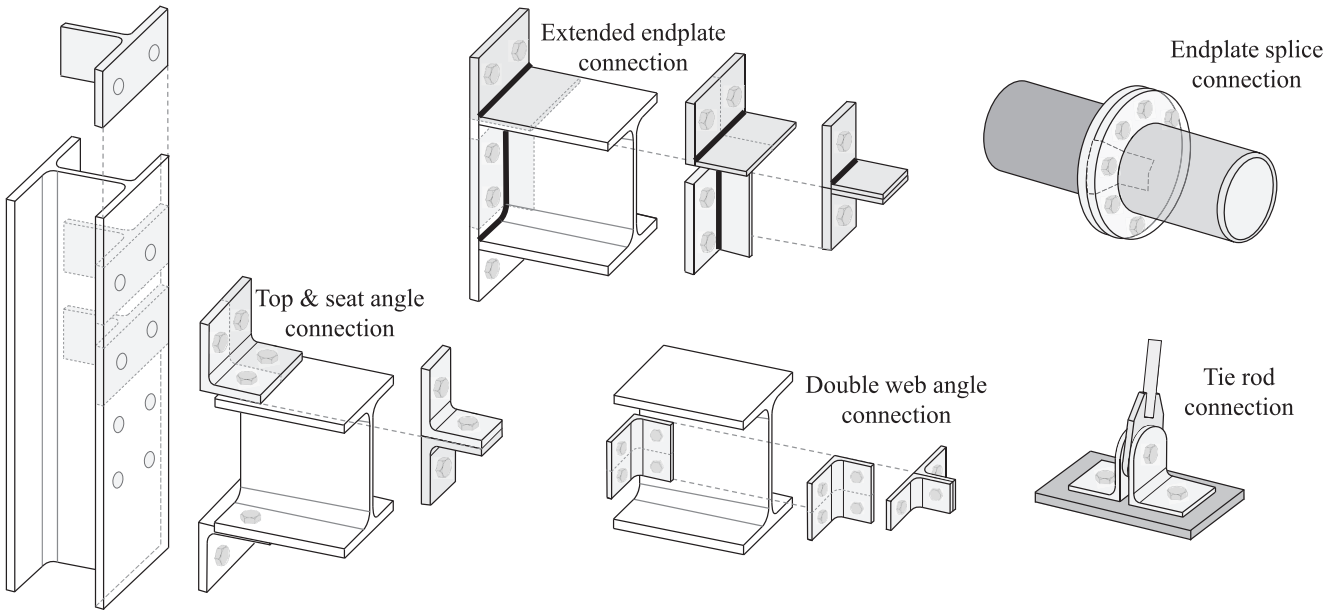

Fig. 1. T-stub components in commonly used bolted steel connections.

Table 1
Summary of test specimens geometry and loading parameters.

No.	ID	Geometry								Preload condition	Loading rate [mm/s]
		b_f	t_f	L_f	t_w	g	p	s	N_{bolt}		
3	T2–6	220	6	80	10	120	–	5	2	ST	0.05; 10; 50
6	T2–8	220	8	80	10	120	–	5	2	ST; FP	0.05; 20; 50
6	T2–10	220	10	80	10	120	–	5	2	FP	0.05; 10; 20
3	T2–10-120	220	10	120	10	120	–	5	2	ST; FP	0.05; 10; 50
3	T2–10D*	220	10	80	10	180	–	5	2	FP	0.1; 40; 100**
5	T2–12	220	12	80	12	120	–	5	2	FP	0.05; 5; 10; 20; 50
6	T2–15	220	15	80	10	120	–	6	2	ST; FP	0.05; 1; 20; 50
4	T2–16	220	16	80	12	120	–	6	2	FP	0.05; 5; 10; 20
6	T2–20	220	20	80	16	120	–	8	2	ST; FP	0.05; 20; 50
6	T4–8	220	8	150	12	120	90	5	4	ST; FP	0.05;1; 10; 50
9	T4–12	220	12	150	12	120	90	6	4	ST; FP	0.05; 5; 10; 20

* Double T-stub configuration.
** The reported speeds represent the separation gap speed (i.e., double that of a single T-stub).

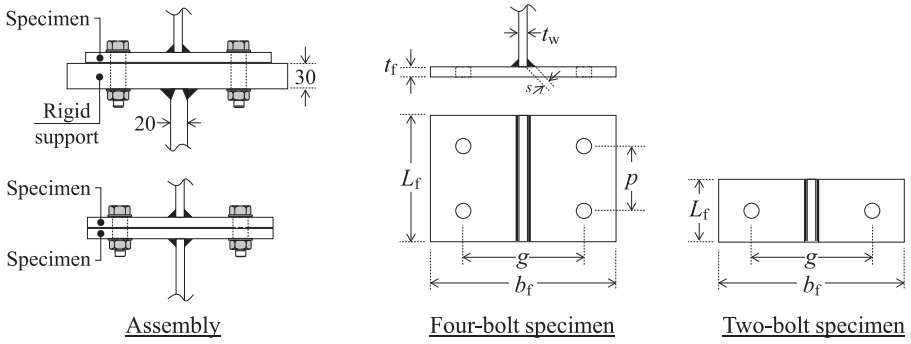

Fig. 2. Schematical diagram of test specimens layout and geometric parameters.

Welding was conducted using the TIG process with a 1.6–2.4 mm filler wire of grade ER70S-2. During welding, measures were taken to ensure a right angle between the welded plates and to minimize flange plate distortion, as shown in Fig. 3. This involved clamping and aligning the plates before welding with temporary tack welds.

2.2. Material properties

Uniaxial monotonic tensile tests were conducted on rectangular coupons extracted from different plate thicknesses. The tests were conducted at different strain rates ranging from 0.002 to 2.0 s^{-1}. For the M16 grade 8.8 bolts, 8 mm round coupon specimens were extracted through a turning-down process. Two tests were conducted for each plate thickness at a given strain rate. The average mechanical material properties are summarized in Table 2. This includes the modulus of elasticity (E), the yield stress (f_y), the ultimate stress(f_u), and the fracture-to-gross area ratio (A_f/A_o). Note that f_y represents the lower yield stress, measured at 0.2% strain offset. The reported stress and strain data are based on the engineering response and an extensometer gauge length of 50 mm and 25 mm for the plate and bolt coupons, respectively.

The dependency of the mechanical properties on the strain rate can be visually investigated using the plots in Fig. 4. In these plots, a dashed line representing the moving average is superimposed. For each plate thickness, the mechanical properties in these plots are normalized by the corresponding value at 0.002 s^{-1} to simplify comparison and discussion. Given that the mechanical properties change almost exponentially, the strain rate axis is shown in the logarithmic scale. The observations are consistent with past tests on mild steel materials [14,29,30]. Specifically, at $\dot{\varepsilon}$ =0.8 s^{-1}, the yield stress is amplified by 13% on average and up to 25%, compared to the reference pseudo-static 0.002 s^{-1} rate (see Fig. 4(a)). Similarly, the ultimate stress is amplified but by a lower factor of 7% (see Fig. 4(b)). Up to 15% reduction is observed in the elastic modulus indicating that it is strain-rate sensitive. With respect to

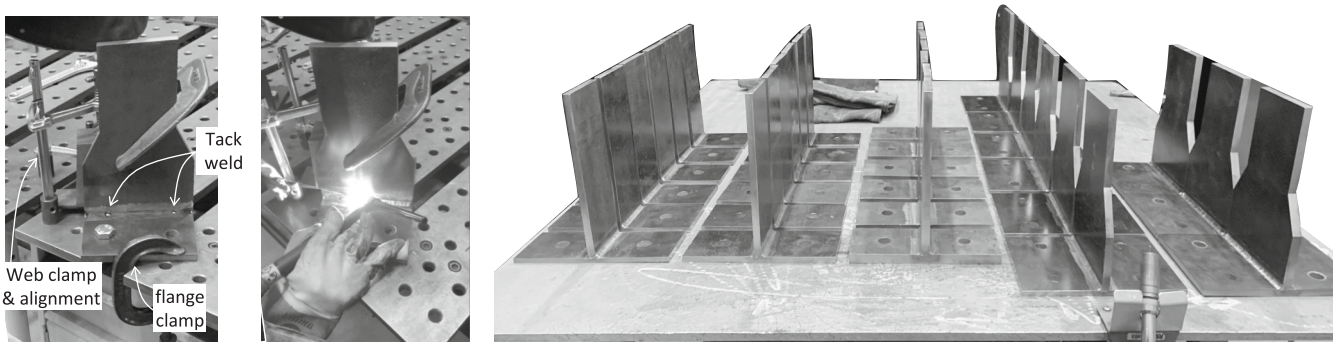

Fig. 3. Test specimens during and after fabrication.

Table 2
Summary of measured material properties.

Plate thickness	Strain rate, $\dot{\varepsilon}$ [s^{-1}]	E [MPa]	f_y [MPa]	f_u [MPa]	ε_u	A_f/A_o
6 mm	0.002	208,079	322	416	0.20	0.28
	0.1	194,835	350	439	0.19	0.33
	0.4	179,608	348	438	0.19	0.32
8 mm	0.002	223,994	341	491	0.15	0.33
	0.1	194,826	363	510	0.15	0.34
	0.4	169.609	379	524	0.14	0.31
	0.8	184,411	393	525	0.14	0.35
10 mm	0.002	202,375	414	525	0.16	0.31
	0.1	207,119	439	541	0.15	0.32
	0.4	190,074	455	555	0.15	0.36
	0.8	172,141	431	541	0.15	0.39
12 mm	0.002	196,212	294	462	0.18	0.29
	0.1	189,957	291	429	0.17	0.30
	0.4	185,229	351	497	0.17	0.31
	0.8	182,903	364	517	0.17	0.31
15 mm	0.002	210,997	248	406	0.22	0.35
	0.1	196,423	296	425	0.19	0.41
	0.4	186,876	315	433	0.19	0.37
	0.8	182,232	286	437	0.20	0.42
	2	180,462	305	442	0.18	0.41
20 mm	0.002	221,041	300	448	0.18	0.34
	0.1	201,604	317	469	0.18	0.34
	0.4	187,810	330	475	0.18	0.35
	0.8	194,083	336	486	0.17	0.34
	2	194,008	333	489	0.17	0.34
M16 Gr 8.8	0.002	197,700	728	914	0.08	0.39
	0.2	171,867	641	821	0.11	0.36
	0.4	158,720	611	821	0.11	0.37

material ductility, about a 10% increase is observed in the A_f/A_o ratio (see Fig. 4(d)), suggesting that the material becomes more brittle at high strain rates. Finally, no notable correlation is observed between all the mechanical properties and the coupon plate thickness; supporting past research observations [29]. For the high-strength grade 8.8 bolt material, different observations are noted where both the yield and ultimate stresses are reduced by about 12% at high strain rates. Others also noted that high-strength steels generally present a less favourable response to the strain rate [29]. The reduction in area at fracture is about 7% higher at $\dot{\varepsilon} = 0.4\ s^{-1}$, indicating a slightly more ductile response for the bolt at high strain rate. More tests are needed however on bolt components to confirm this observation, since others noted an opposite effect on ductility [14].

2.3. Experimental setup

The tests were conducted in the Testing and Structural Research Laboratory (TSRL) at the University of Southampton, using a 630kN Schenck servo-hydraulic machine, as shown in Fig. 5(a). The test specimens were tested in a T-stub to rigid support and double T-stub configurations (see Fig. 5(b)). A series of steps were followed in each test. First, the web of the rigid support (or that of the lower T-stub in the case of the double-configuration specimens) is clamped to the machine's actuator. The rigid support surface was checked before each test to confirm the absence of distortion and to ensure levelness. Second, the T-stub specimen is centred relative to the rigid support, the bolt holes are aligned and then tightened to the snug-tight or fully preloaded condition. This is done using a gauged torque wrench as shown in Fig. 5(c). For the snug-tight condition, the bolts were tightened up to a torque of 80 N.m. For the fully-preloaded condition, a 280 N.m torque is used which corresponds to a preload force of about 88kN per bolt (70% of bolt nominal ultimate tensile resistance), assuming a nut (k) factor equal to 0.20. Full preloading was conducted in two passes (and in a cross pattern in the case of the 4 bolt specimens) to ensure the preload was evenly distributed. Lastly, the T-stub specimen's web is clamped to the machine's crosshead, and tensile loading is applied at the specified loading rate shown in Table 1 up to complete failure. A two-dimensional Digital Image Correlation (DIC) system was employed for all specimens to provide a redundant system for capturing deformations and to investigate the progression of local plastic strains. The DIC measurements were also used to deduce the specimen deformation accurately while omitting

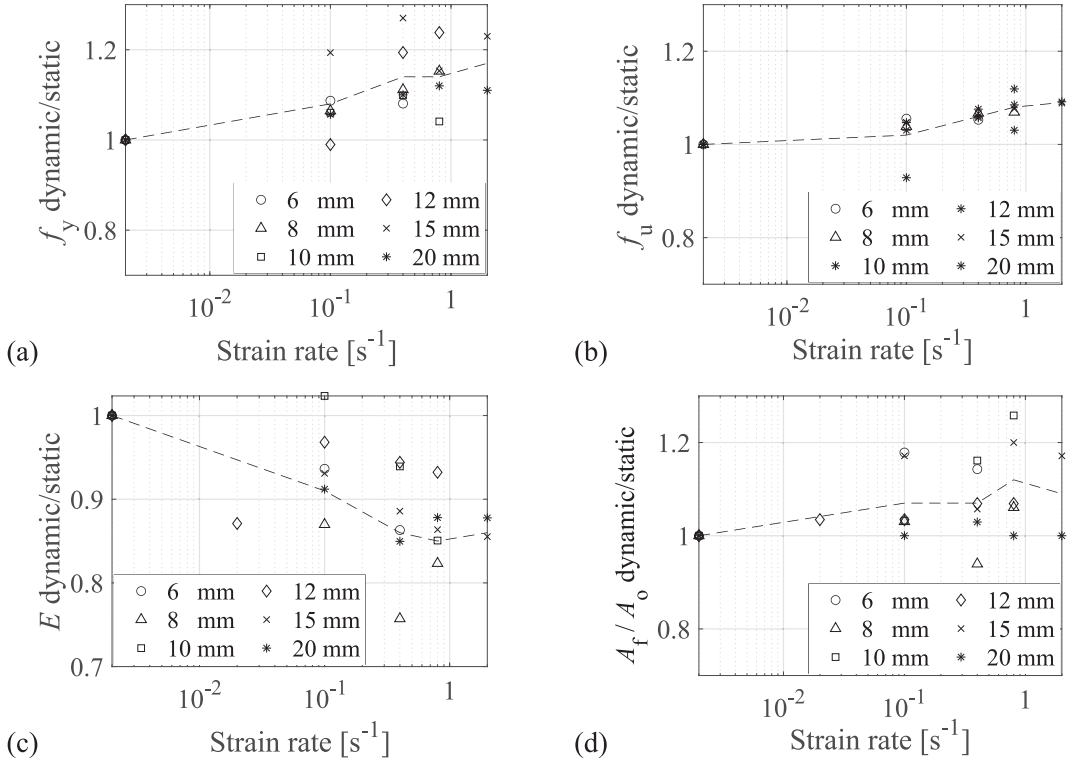

Fig. 4. Normalized mechanical properties for S275 material versus strain rate.

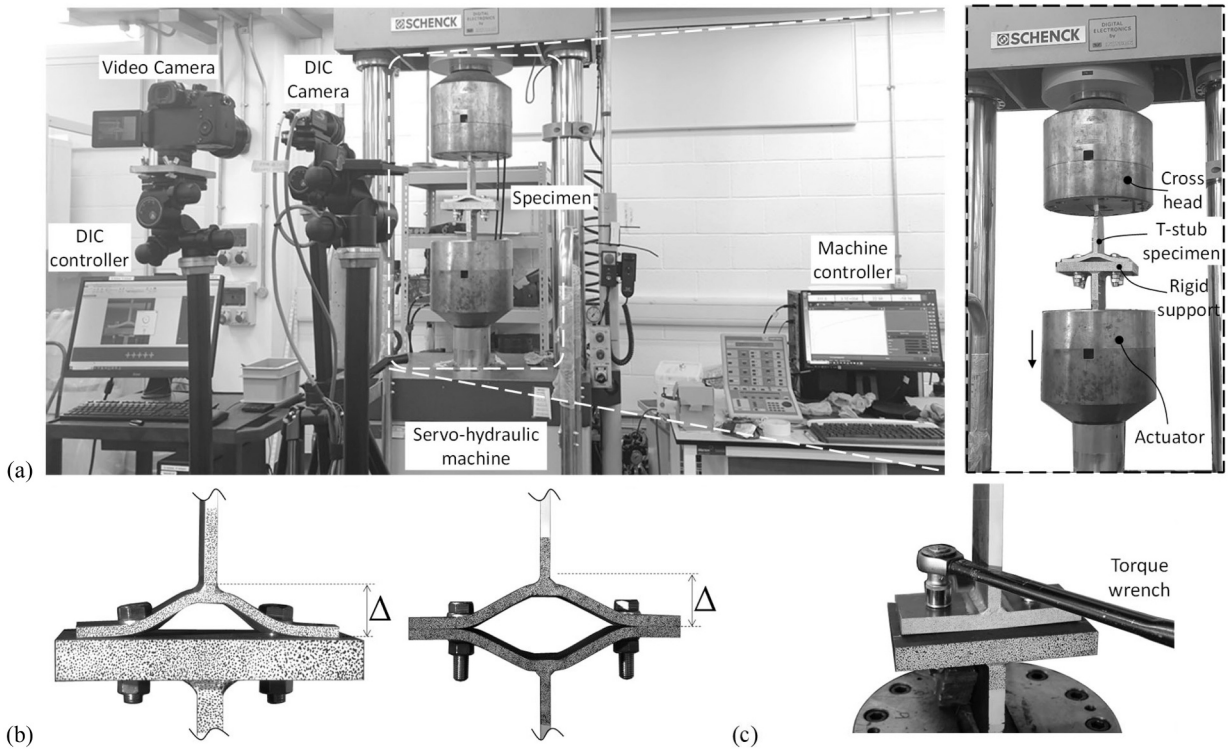

Fig. 5. (a) Test setup for T-stub testing; (b) Specimen types and deformation measurement; (c) Bolt tightening with a torque wrench.

any potential slip in the clamps or elastic deformations in the web.

3. Discussion of results

3.1. Overall response and deformation modes

The force-deformation curves for all specimens are plotted in Fig. 6. To simplify the discussion, separate figures are provided based on the flange plate thickness and the bolt preload case, in which the individual responses at the different loading rates are compared. In these plots, the deformation represents the separation gap between the T-stub specimen and the rigid support. In the case of the double T-stub specimens, this deformation represents half of the separation gap (i.e., the deformation of a single T-stub component), as demonstrated in Fig. 5(b). For reference, the plastic strength as per Eurocode 3 Part 1–8 [1], $F_{p,\ Rd}$, is computed using the measured pseudo-static material properties and no partial safety factor, and superimposed in the same plots.

Fig. 7(a) shows images of the deformation mode for the two-bolt specimens, with different flange thicknesses, right before failure. The Von Mises equivalent strain contours are superimposed in those images, as computed by the DIC system. The deformation mode depends on the flange plate thickness, as expected. The thin 6 mm and 8 mm T-stubs are governed by flange bending where double plastic hinging takes place near the weld toes and the bolt (corresponding to *Mode 1* as per CEN [1] classification). This is followed by the onset of the membrane action (plate axial tension) and bolt hole elongation under larger deformations. The force-deformation response of these specimens is characterized by the onset of the membrane action, evident by the sudden increase in the post-yield slope following flange bending. The sudden increase in force resulted in two failure modes: a) bolt rupture under combined tension-shear and b) weld fracture under increasing tensile strains at the weld toe [31]. The membrane action diminishes with thicker 10 mm and 12 mm flange plates. The thick 15 mm to 20 mm T-stubs are governed by flange yielding at the weld toe. Increased prying action leads to increased bolt elongation and eventually tensile rupture (corresponding to *Mode 2* as per CEN [1] classification). Most of the tests failed to bolt rupture as the photo in Fig. 7(b) shows. The photo also shows the two types in which bolt rupture manifested: 1) bolt shank rupture under combined shear and tension, and 2) necking followed by bolt thread rupture under tension. The former is observed in thinner specimens while the latter is observed in thicker specimens. Twelve tests failed by weld failure near the weld toes as can be seen in Fig. 7(c). This primarily took place in the more flexible T-stub specimens (T2–6-80 and T2–8-80D). The heat-affected zone (HAZ) near the weld toe in those thin/flexible specimens is more prone to fail under larger tensile strains imposed by the membrane action. Only one specimen failed due to bolt thread stripping. This was due to the incorrect usage of the proper nut grade.

To quantitatively evaluate the effect of the bolt preload and loading rate on the T-stub behaviour, response quantities are numerically deduced from the force-deformation data using the procedure described in Elkady [32]. Each response quantity, namely the elastic stiffness, ultimate strength, and ductility, is discussed in the subsequent subsections.

3.2. Elastic stiffness

The T-stub elastic stiffness is one of the most fundamental quantities used to quantify the global joint stiffness. This is detrimental in classifying the joint rigidity and in the consequent design process. Fig. 8 shows a comparison of the measured elastic stiffness, K_e, for the T-stub specimens. To simplify the visualization and comparison in Fig. 8, the stiffness values for each group of T-stub specimens (with the same t_f) are normalized with that of the specimen with pseudo-static loading (i.e., 0.05 mm/s) and snug-tight condition (if applicable). The effect of bolt preload is evident in this plot for all cases. Specimens with fully pre-loaded bolts develop an elastic stiffness that is, on average, 1.75 times larger than that of a snug-tight specimen. This amplification can be as high as four times, consistent with past observations [18–20]. Generally, the bolt preload will have a lower impact on thin T-stubs, considering that those are controlled by flange bending in double curvature where the prying force is small. One should also note that the absolute value of

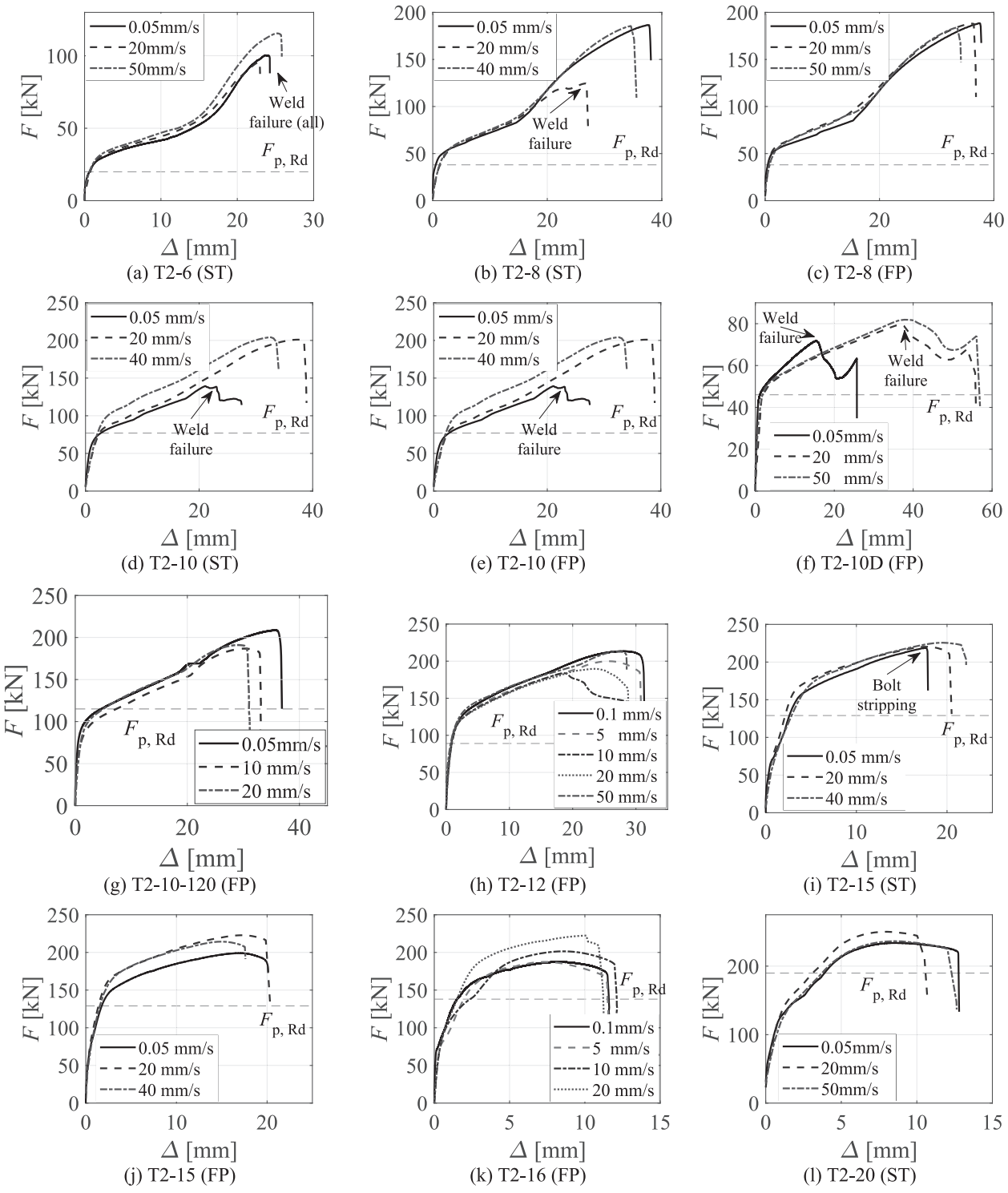

Fig. 6. Force-deformation plots for the tested specimens.

the stiffness is sensitive to the flange plate's initial imperfection (distortion due to welding) which is more evident in thicker plates [33–36].

The reduction in the elastic stiffness with higher loading rates is also evident in the bar plot. This is further investigated through Fig. 9 which shows K_e, normalized by the pseudo-static K_e, as a function of t_f. An average of 35% reduction in K_e is observed compared to the 0.05 mm/s case. This is consistent with the reduction level in the elastic modulus that is observed from the material tests. The reduction in stiffness can also be attributed to the loss of -static- friction under high-velocity loading. This is consistent with past research by Suita et al. [2] that noted a 50% drop in friction forces at high loading rates of 4 mm/s. Notwithstanding the uncertainty and sensitivity associated with K_e, a clear trend is also noticeable concerning t_f (refer to the trend line in Fig. 9), where the reduction in stiffness under high loading rates is more evident in thinner plates. The reduction in stiffness can be as high as 80% in thin plates. Finally, the preload did not seem to significantly alter the observed loading rate effect. However, in couple of cases (e.g.,

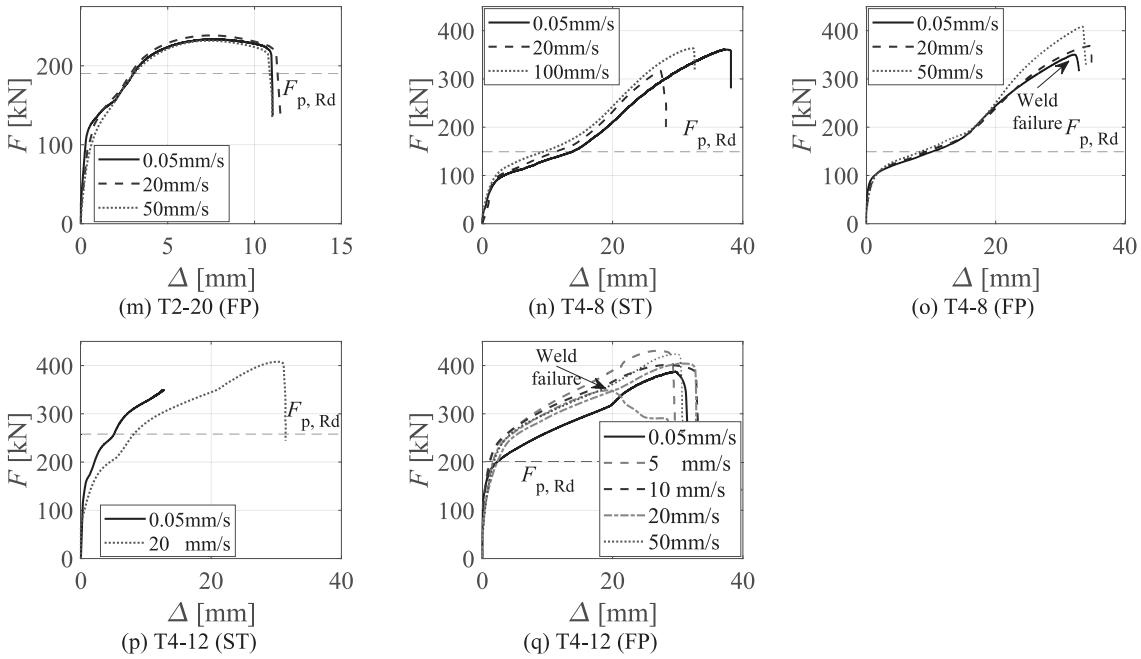

Fig. 6. (*continued*).

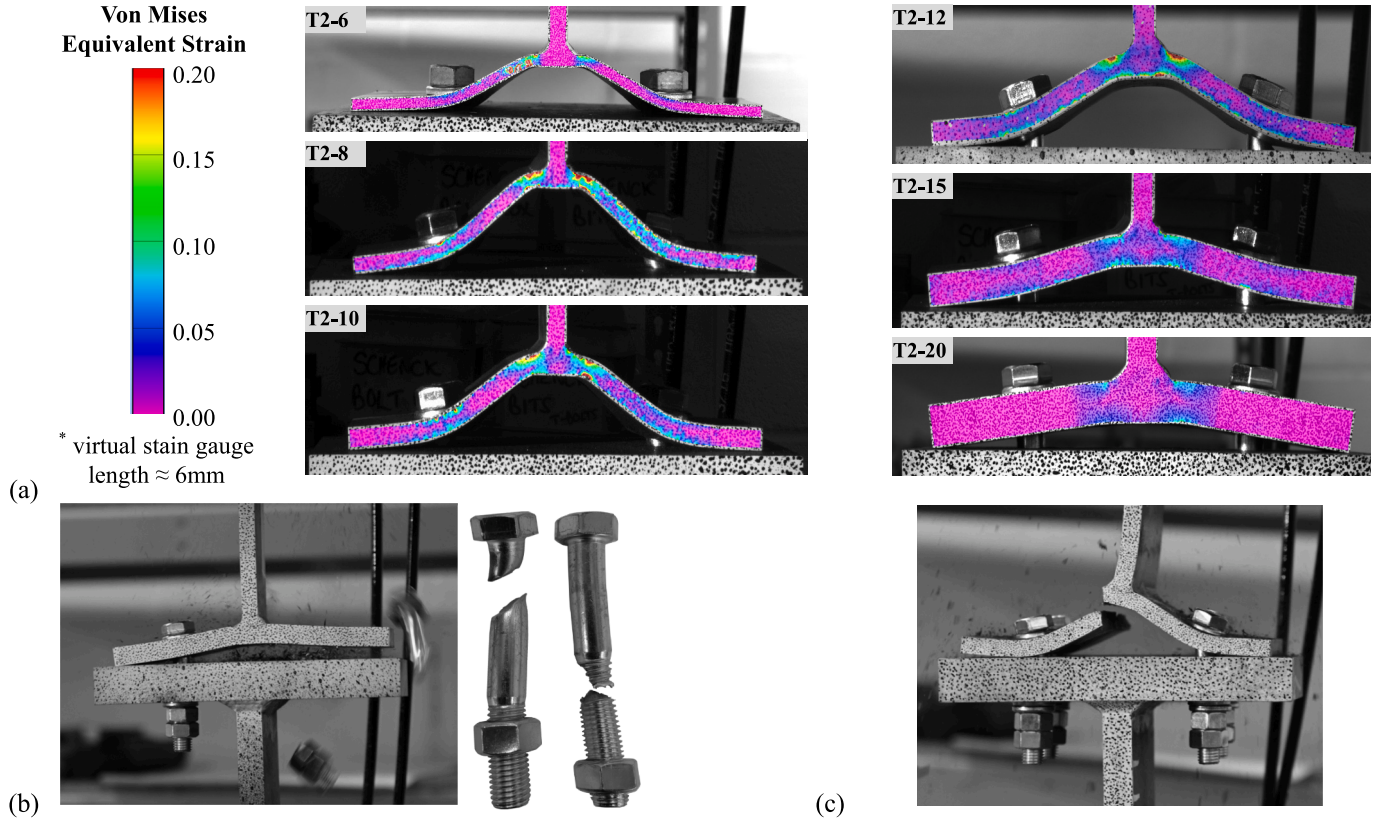

Fig. 7. (a) Deformation modes, right before failure, and corresponding Von Mises strain distribution for 2-bolt T-stubs with different thicknesses; Photos of the observed failure modes: (b) bolt rupture and (c) weld failure.

T2–20 and T4–8), the loading rate effect on stiffness was more pronounced in the preloaded cases. In fully preloaded specimens, static friction is a key feature that reduces slippage and consequently increases stiffness. When this feature is lost under high-speed loading, the drop in stiffness may become pronounced. The observed reduction in ductility at the component-level will potentially extend to affect the elastic rotational stiffness at the joint-level (e.g., as part of pre-qualified extended endplate connections). A reduced joint stiffness under dynamic load (e.g., an earthquake) will lengthen the structural period and may affect both the global force distribution and drift demands. This deserves

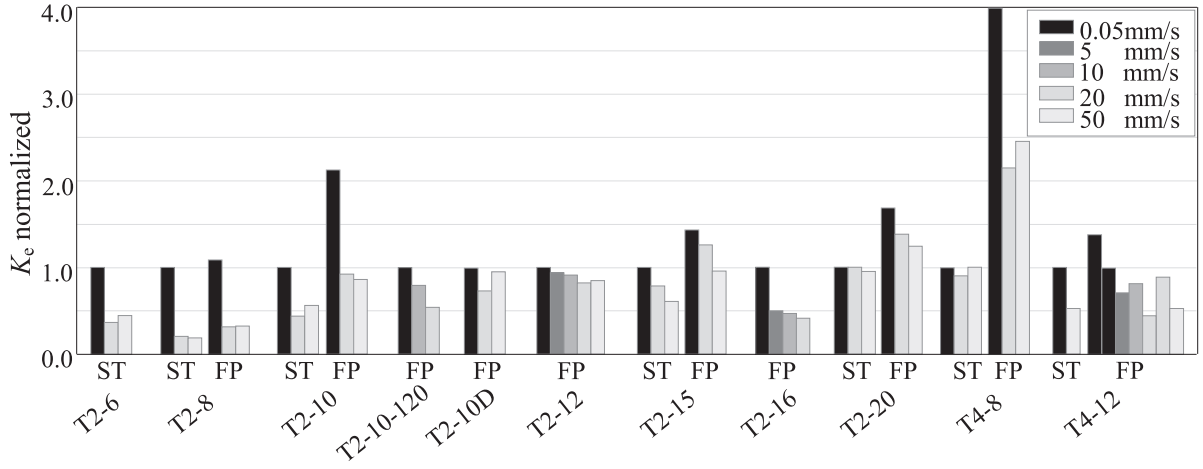

Fig. 8. Comparison of the normalized elastic stiffness.

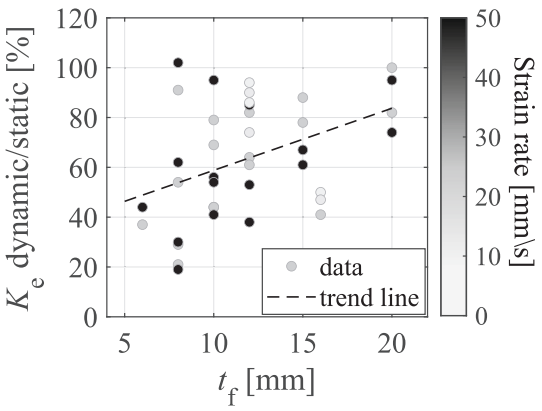

Fig. 9. Relation between reduction in stiffness under high loading rates and the plate thickness.

further investigation.

3.3. Plastic and ultimate capacity

Past research mostly reported an increase in the strength of bolted components and joints at high strain rates [24–27]. This is investigated in this section using the deduced ultimate force, F_u. Specimens that failed due to weld failure are excluded from the consequent discussion and computed statistics since those represent premature failure. Referring to Fig. 10, the bolt preload condition seems to have no effect on the ultimate capacity of the T-Stub, with an FP-to-ST force ratio ranging between 0.95 and 1.12. The loading rate seems to have a minor effect where an average 5% amplification is observed in F_u. However, this amplification is inconclusive. That may be due to the reverse effect the strain rate had on the ultimate stress of the plate and bolt materials, as discussed earlier. One should note that similar observations can also be driven about the plastic capacity of the T-Stubs, as inferred from Fig. 6.

The plastic capacity of the T-stubs is deduced using an equal-area fitting method (refer to [32]). The values are used to assess the plastic design values ($F_{p,Rd}$) predicted by Eurocode 3 Part 1–8 [1]. Fig. 11(a) shows the scatter for the test-to-theoretical ratio, where $F_{p,Rd}$ is computed using the pseudo-static material properties. Fig. 11(b) is based on $F_{p,Rd}$ which is computed using the actual material properties corresponding to each test loading rate. When using the pseudo-static material properties, the average ratio is about 1.13, indicating that Eurocode 3 will be underestimating the resistance by 13% on average. This is expected given that the material -at least of the plate steel- possesses enhanced strength under high strain rates. If the proper (i.e., loading rate representative) material properties are used, the average ratio drops down to 1.03. This is evident in Fig. 11(b) where high loading-rate data points move closer to unity. In design, this can simply be done using prespecified material modification factors. This is critical to avoid altering the damage/failure model stipulated in the design process, particularly in finely tuned bolted joints. It is worth noting that although the prediction error is reduced -on average- in Fig. 11(b), it appears that the Eurocode 3 approach tends to underestimate the plastic capacity for thin flange T-stubs by about 40% and overestimate that of thick flange plates by about 35%. This can be attributed to the assumptions used by the Eurocode 3 method, including the discretization of the T-stub deformation shape into three modes, and the idealization of the flange plate yield lines associated with each mode. This type (and level) of prediction errors is well documented in the literature where several researchers have proposed more accurate variations of this approach [37,38].

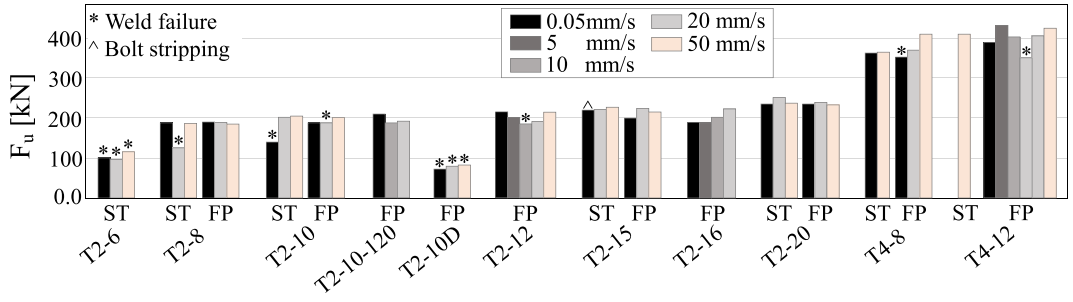

Fig. 10. Comparison of the ultimate capacity.

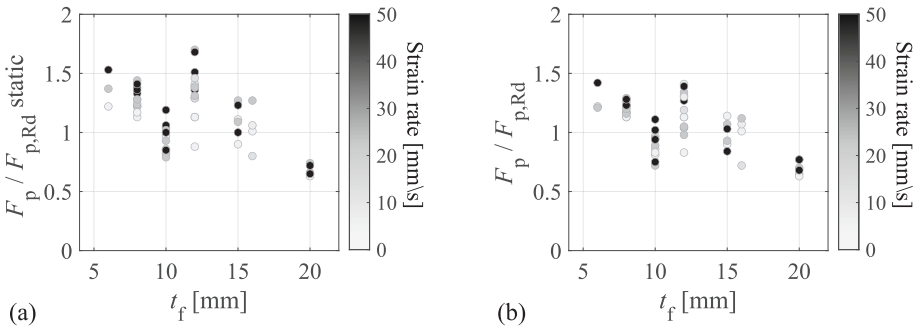

Fig. 11. Measured versus design plastic capacity per [1] versus flange thickness, using (a) pseudo-static material properties, and (b) strain-rate representative material properties.

3.4. Ductility

The T-stub ductility is quantified using the deformation at failure, Δ_f. As shown in Fig. 6, this coincides with the ultimate force (i.e., capping point). The bar plot in Fig. 12 compares Δ_f for all tests. As expected from past research, a clear inverse correlation is observed between the specimen ductility and its flange plate thickness. This is already noticeable from the deformation mode in Fig. 7. The thin 8 mm and 20 mm T-stubs deform by about 38 mm and 12 mm, respectively. Assuming these T-stubs are part of a beam-to-column joint with an extended endplate connection and a 500 mm deep beam, this transforms to a joint rotation capacity of 7.6% and 2.4%, respectively. The 8 mm T-stub ductility is further amplified by 58% when the bolt gauge length is increased by 50%, from 120 mm to 180 mm (i.e., specimen T2–10D). The 6 mm specimens are excluded from the observed Δ_f-t_f correlation. This is due to the occurrence of significant bolt-hole elongation under increasing membrane forces, which eventually leads to weld failure. No notable difference in ductility between two- and four-bolt specimens of the same thickness.

Excluding specimens failing by weld failure, Fig. 12 demonstrates another inverse correlation between ductility and loading rate. At 50 mm/s, ductility appears to be reduced by about 6% to 22%, compared to the pseudo-static 0.05 mm/s loading rate. This effect seems to diminish and become unclear in thick T-stubs with t_f larger than 15 mm. This may be attributed to the fact that these plates are more controlled by bolt tensile elongation and are more affected by other factors such as bolt preload and the initial distortion of the flange plate. Finally, contrary to past research [18], no consistent tendency is observed between ductility improvement and bolt preload across all flange plate thicknesses.

4. Summary and conclusions

A total of 57 welded T-stub specimens were tested with different flange plate thicknesses and number of bolt rows. The aim is to generate unique test data for T-stub components, with different preload conditions, undergoing varying loading rates (up to 50 mm/s) that can potentially help in a clearer understanding of high loading/strain rates effects on the mechanical properties of T-stubs. This data addresses the limited number of high-speed/dynamic tests on bolted steel joints/components. The following experimental observations are made:

- Material coupon tests provided consistent findings to those found in the literature. Specifically, for grade S275 steel, the yield and ultimate stresses are amplified on average by 13% and 7%, respectively when subjected to a strain rate of 2 s^{-1}. At the same strain rate, a 15% reduction in the modulus of elasticity is observed. The material also demonstrates brittleness (−10% reduction in ductility) with high strain rates. Opposite observations are made with respect to strength and ductility, for the high-strength grade 8.8 bolt material.
- The T-stubs deformed according to Eurocode 3 *mode 1* and *mode 2*. Thin flange plate (≤8 mm) experienced plate bending in double curvature, bolt-hole elongation, and significant membrane action. Thick flange plate (≥15 mm) experienced plate yielding near weld toe and bolt elongation followed by bolt tensile rupture. Weld failure was more evident in thin T-stubs and more probable under high loading rates.
- Among the different mechanical properties, the elastic stiffness is the most affected by both the bolt preload and the loading rate. Bolt preload improved the stiffness by up to four times. On the other hand, the stiffness is reduced by about 35% under high loading rates owing to slippage and the reduced materials' elastic modulus. This reduction was more evident in thinner T-stubs.
- The bolt preload did not affect either the plastic or ultimate capacities of the specimens. The loading rate had a rather minor effect. At 50 mm/s, an average 5% increase in the ultimate resistance is observed. This amplification, which is driven by the enhanced material properties, can be as high as 15%. However, there is a notable uncertainty associated with this amplification factor.
- Eurocode 3 Part 1–8 plastic strength prediction can be generally improved if true strain-rate-dependant material properties are used

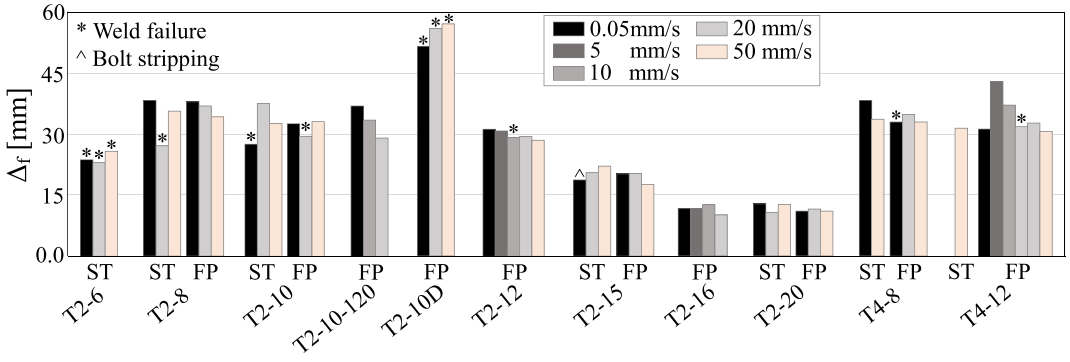

Fig. 12. Comparison of T-stub specimens' deformation at failure.

in the computation. Otherwise, the code prediction is on the conservative side by 13% on average. Regardless, a ± 40% error is still evident due to the analytical assumptions of the code approach.

- The bolt preload did not affect the T-stub ductility. Conversely, the ductility is shown to be inversely proportional to the loading rate. Failure may occur 22% earlier under higher loading rates. This is more evident in thinner specimens. This impact on ductility can be more pronounced under rapid cyclic loads as those experienced during an earthquake. Therefore, more stringent ductility limits may be required for the design of steel joints. Relevant damage fragility curves should be revised as well since this affects the estimated damage and its consequences (e.g., collapse/demolition probability and repair time/cost) within the performance-based engineering framework [39]. This particularly includes partial-strength joints (with relatively thin components and fillet welding) that are typically employed as part of the secondary gravity-framing systems.
- The presented experimental study provides important insights into the potential effects of high loading/strain rates on the performance of steel components. The presented findings are valid for the material grades used in this experimental campaign (i.e., S275 and Gr 8.8) and the welding grade/procedure. For other material grade combinations, the observations may vary. The results may be dependent as well on other factors such as the bolt finish/coating type, the amplitude of residual stresses and the plate distortion resulting from the welding procedure, particularly in the thicker plates. Further experimental research is required to assess the role of these aspects on the T-stub response and to better understand the load/strain rate phenomena and the associated uncertainty. Finally, more dynamic tests are needed to investigate how do the component-level observations herein scale at both the joint- and system-levels.

CRediT authorship contribution statement

Grace Kendall: Writing – original draft, Visualization, Investigation, Formal analysis, Data curation. **Artem Belyi:** Writing – original draft, Visualization, Investigation, Formal analysis, Data curation. **Ahmed Elkady:** Writing – review & editing, Visualization, Supervision, Resources, Methodology, Conceptualization.

Declaration of competing interest

The authors declare that they have no known competing financial interests or personal relationships that could have appeared to influence the work reported in this paper.

Data availability

The experimental database upon which the current work is based can be made available from the corresponding author upon reasonable request.

Acknowledgements

This work was conducted at the National Infrastructure Laboratory, University of Southampton (UoS). The authors gratefully acknowledge the financial support provided by UoS to the first and second authors as part of their studentship project. The authors would like to thank the Testing and Structures Research Laboratory (TSRL) staff, particularly Aga Murch, Andrew Morgan, and Stuart Findlow, for their technical assistance throughout the testing program, as well as former master students Zihan Li and Yan Yan for their support in the first phase of testing.

References

[1] CEN, Eurocode 3 - Design of Steel Structures, Part 1–8: Design of Joints, European Committee for Standardization, Brussels, Belgium, 2005.
[2] K. Suita, K. Kaneta, I. Khozu, The effect of strain rate in steel structural joints due to high speed cyclic reversed loadings, in: 10th World Conference on Earthquake Engineering, Rotterdam, Netherlands, 1992, pp. 137–145.
[3] P.S.B. Shing, S.A. Mahin, Rate-of-loading effects on Pseudodynamic tests, J. Struct. Eng. 114 (11) (1988) 2403–2420.
[4] D. Forni, B. Chiaia, E. Cadoni, Strain rate behaviour in tension of S355 steel: base for progressive collapse analysis, Eng. Struct. 119 (2016) 164–173.
[5] P. Soroushian, K.-B. Choi, Steel mechanical properties at different strain rates, J. Struct. Eng. 113 (4) (1987) 663–672.
[6] A.A. Alabi, P.L. Moore, L.C. Wrobel, J.C. Campbell, W. He, Influence of loading rate on the fracture toughness of high strength structural steel, Procedia Struct. Integr. 13 (2018) 877–885.
[7] C.S. Wiesner, H. MacGillivray, Loading Rate Effects on Tensile Properties and Fracture Toughness of Steel, Fracture, Plastic Flow and Structural Integrity, CRC Press, 2019, pp. 149–174.
[8] K. Wallin, Fracture Toughness of Engineering Materials: Estimation and Application, EMAS Publishing, 2011.
[9] D. Dubina, A. Stratan, Behaviour of welded connections of moment resisting frames beam-to-column joints, Eng. Struct. 24 (11) (2002) 1431–1440.
[10] A. Al-Rifaie, Z.W. Guan, S.W. Jones, Q. Wang, Lateral impact response of end-plate beam-column connections, Eng. Struct. 151 (2017) 221–234.
[11] E.L. Grimsmo, A.H. Clausen, M. Langseth, A. Aalberg, An experimental study of static and dynamic behaviour of bolted end-plate joints of steel, Int. J. Impact Eng. 85 (2015) 132–145.
[12] A. Elkady, L. Mak, Data driven evaluation of existing numerical modelling guidelines for semi-rigid connections, in: 10th International Conference on Behaviour of Steel Structures in Seismic Areas (STESSA), Springer International Publishing, Timisoara, Romania, 2022, pp. 244–251.
[13] Z. Ding, A. Elkady, Semirigid bolted end-plate moment connections: review and experimental-based assessment of available predictive models, J. Struct. Eng. 149 (9) (2023).
[14] G. Culache, M.P. Byfield, N.S. Ferguson, A. Tyas, Robustness of beam-to-column end-plate moment connections with stainless steel bolts subjected to high rates of loading, J. Struct. Eng. 143 (6) (2017) 04017015.
[15] F. Dinu, D. Dubină, I. Marginean, C. Neagu, I. Petran, Structural connections of steel building frames under extreme loading, Adv. Mater. Res. 1111 (2015) 223–228.
[16] N. Baldassino, M. Bernardi, R. Zandonini, Experimental and Numerical Analyses of the Loading Rate Influence on the T-Stub Response, Università degli Studi di Trento, Trento, Italy, 2017, pp. 50–56.
[17] Y. Cai, B. Young, Experimental investigation of carbon steel and stainless steel bolted connections at different strain rates, Steel Compos. Struct. 30 (6) (2019) 551–565.
[18] Y. Zhang, S. Gao, L. Guo, J. Qu, S. Wang, Ultimate tensile behavior of bolted T-stub connections with preload, J. Build. Eng. 47 (2022) 103833.
[19] J.-P. Jaspart, R. Maquoi, Effect of bolt preloading on joint behaviour, in: 1st European Conference on Steel Structures, Athens, Greece, 1995, pp. 219–226.
[20] C. Faella, V. Piluso, G. Rizzano, Experimental analysis of bolted connections: snug versus preloaded bolts, J. Struct. Eng. 124 (7) (1998) 765–774.
[21] A. Tyas, J.A. Warren, E.P. Stoddart, J.B. Davison, S.J. Tait, Y. Huang, A methodology for combined rotation-extension testing of simple steel beam to column joints at high rates of loading, Exp. Mech. 52 (8) (2012) 1097–1109.
[22] R. Rahbari, A. Tyas, J.B. Davison, E.P. Stoddart, Web shear failure of angle-cleat connections loaded at high rates, J. Constr. Steel Res. 103 (2014) 37–48.
[23] H. Wang, K.H. Tan, B. Yang, Impact resistance of steel frames with different beam-column connections subject to falling-floor impact on various locations, J. Struct. Eng. (United States) 147 (4) (2021).
[24] K. Suita, M. Nakashima, K. Morisako, Tests of welded beam-column subassemblies. II: detailed behavior, J. Struct. Eng. 124 (11) (1998) 1245–1252.
[25] K. Udagawa, K. Takanashi, B. Kato, Effects of displacement rates on the behavior of steel beams and composite beams, in: 8th World Conference on Earthquake Engineering, San Francisco, CA, USA, 1984, pp. 177–184.
[26] A. El Hassouni, A. Plumier, A. Cherrabi, Experimental and numerical analysis of the strain-rate effect on fully welded connections, J. Constr. Steel Res. 67 (3) (2011) 533–546.
[27] Y. Chen, J. Huo, W. Chen, H. Hao, A.Y. Elghazouli, Experimental and numerical assessment of welded steel beam-column connections under impact loading, J. Constr. Steel Res. 175 (2020) 106368.
[28] ISO 4014, Fasteners – Hexagon head bolts – Product grades A and B, in: DIN 931/EN ISO 4014: 2022–10, International Organization for Standardization, Geneva, Switzerland, 2022.
[29] M.F.D.F. Pereira, Robustness of Multi-Storey Steel-Composite Buildings under Column Loss: Rate-Sensitivity and Probabilistic Framework, Department of Civil and Environmental Engineering, Imperial College London, London, UK, 2012.
[30] K. Kawata, A new testing method for the characterization of materials in high velocity tension, Mechan. Prop. High Rates Strain 1979 (1979) 71–80.
[31] J. Goltz, The Northridge, California Earthquake of January 17, 1994: General Reconnaissance Report, National Center for Earthquake Engineering Research (NCEER), New York, USA, 1994.
[32] A. Elkady, Response characteristics of flush end-plate connections, Eng. Struct. 269 (2022).

[33] O. Yapici, Advanced finite element modelling of stainless steel bolted T-stubs under large deformations, Structures 58 (2023) 105461.
[34] R. Tartaglia, M. D'Aniello, M. Zimbru, Experimental and numerical study on the T-stub behaviour with preloaded bolts under large deformations, Structures 27 (2020) 2137–2155.
[35] A.P. Mann, L.J. Morris, Significance of Lack of Fit-Flush Beam-Column Connections, Joints in Structural Steelwork, Pentech Press, London, 1981, pp. 6.22–6.36.
[36] T. Mineyama, Research on Rationalization of Bridge Member Connection Structure Using High-Strength Bolt Tensile Joints (in Japanese), Graduate School of Engineering, Osaka City University, Osaka, Japan, 2020.
[37] A.M.G. Coelho, Characterization of the Ductility of Bolted End Plate Beam-to-Column Steel Connections, Department of Civil Engineering, University of Coimbra, Coimbra, Portugal, 2004.
[38] A.C. Faralli, M. Latour, P.J. Tan, G. Rizzano, P. Wrobel, Experimental investigation and modelling of T-stubs undergoing large displacements, J. Constr. Steel Res. 180 (2021) 106580.
[39] FEMA, Seismic Performance Assessment of Buildings, Federal Emergency Management Agency, Washington, DC, 2012.